APPENDIX S1: DESCRIPTION OF THE ESTIMATION OF THE VARIANCES OF OUR MAXIMUM LIKELIHOOD ESTIMATORS

For large *n*, the negative inverse of the second derivative of the likelihood function at the optimum can be used as an estimate of the variance of the maximum likelihood estimator. This is a very intuitive property of likelihood functions: the flatter the likelihood surface, the less negative the curvature at the maximum, and thus the larger the negative derivative (and vice versa). Unfortunately, the likelihood functions in our study were not readily differentiable, and as a consequence we estimated our ML parameter values numerically. However, we would nonetheless like to obtain sampling variances for our estimates. We accomplished this by fitting a quadratic approximation to the likelihood surface at the optimum. We then computed the second derivative and its negative inverse, to estimate the variance of our MLE. For our bivariate ML optimization (of σ_0^2 and ψ), we held one parameter constant, and fit the quadratic approximation to the other. Since this analysis was computationally and labor intensive, we computed estimation variances of our MLEs only for the MCC tree.

To combine our MLE parameter estimation variance with error variance associated with phylogenetic uncertainty, we simply assumed that the variances were independent and added them. The square roots of these summed error variances are reported in Table 2 as standard errors.

APPENDIX S2: EXTINCTION AND METHOD PERFORMANCE

A difficulty with phylogenetic comparative methods that investigate historical ecological patterns is that they typically cannot accurately account for the influence of unknown extinct taxa. Our models assume that extinction did not occur.

In this section, we discuss this assumption both generally and for Greater Antillean anoles, and then we describe a simulation study we conducted to evaluate the performance of our methods under a wide range of extinction scenarios. The results of this study also provide a useful general performance evaluation of our methods for identifying the signature of historical ecological opportunity in comparative data.

The potential influence of extinction on patterns of lineage diversification and phenotypic evolution:

Extinction is problematic for phylogenetic comparative studies of extant taxa because it is difficult to estimate its influence using phylogenetic data alone (despite the existence of comparative methods for such estimation; Kubo and Iwasa 1995; Quental and Marshall 2009; Rabosky 2009a, 2010). The influence of extinction on estimates of lineage diversification rates has recently been the subject of considerable interest, as accurate estimation of rates of cladogenesis depends critically on realistic estimation of extinction rates (Nee et al. 1994; Marshall 2007; Bokma 2009; Quental and Marshall 2009; Rabosky 2009a, 2010).

The expected effects of extinction on phenotypic rate estimates, however, are distinct from the slightly more insidious effects on estimates of lineage diversification. The Brownian motion null model of phenotypic evolution has the desirable property of exhibiting constant expected variance in standardized contrast values for traits regardless of tree topology (Felsenstein 1985). Extinction is problematic for studies of lineage diversification because it affects estimates of tree shape, and lineage diversification studies extract important parameter values from tree shape (Mooers and Heard 1997). In contrast, for studies of phenotypic rates, misestimation of tree shape due to unrecorded extinction is not expected to create bias in the null expectation of constant phenotypic variance through time.

Of course, failing to sample extinct lineages from deep within the tree will still cause underestimation of historical lineage diversity values at these nodes. This problem will be less important when the number or proportion of missing lineages is similar through time (because lineage diversity estimates will be strongly correlated with historical patterns, if not absolutely concordant) and more important in cases in which extinction rates varied widely between the origin of a group and the present.

Due to a paucity of fossils, we do not presently know what the history of lineage extinction has been for the radiation of Greater Antillean anoles. All known pre-Late Pleistocene Greater Antillean fossils from this radiation originate from a single mid-Miocene amber deposit (15-25 mya), and are assignable to a single known extant lineage (Rieppel 1980; de Queiroz et al. 1998; Polcyn et al. 2002), but we cannot rule out the possibility that major undiscovered lineages were present in the past. The phylogenetic
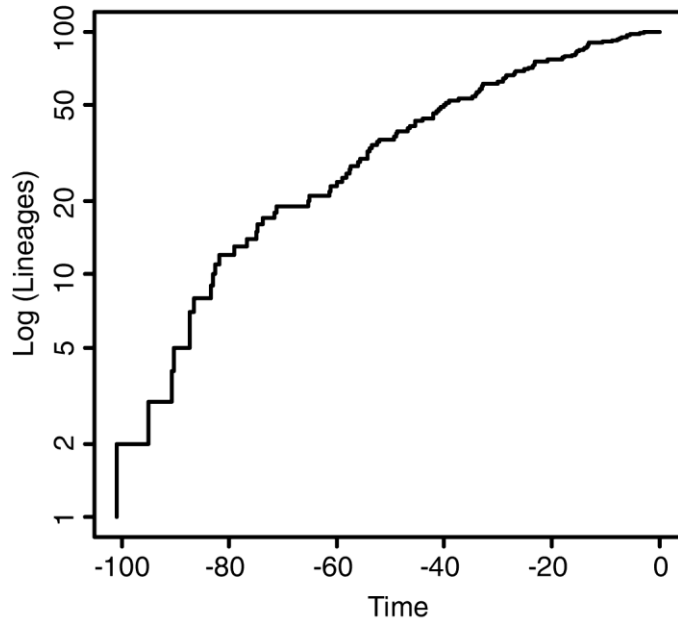

Figure S1. Lineages-through-time plot for the Greater Antillean *Anolis* radiation, using the Bayesian MCC topology.

pattern of Greater Antillean anole diversification was one of extraordinarily rapid early diversification, followed by a slowdown in lineage accumulation (γ = -5.07; Pybus and Harvey 2000; Figure S1), which is consistent with a model of explosive radiation accompanied by low extinction rates (Rabosky and Lovette 2008a). However, several alternative models have recently been proposed that could also explain such a phylogenetic pattern, and some of these models may include substantial extinction (McPeek 2008; Bokma 2009; Quental and Marshall 2009; Rabosky 2009a,b).

Simulation of phenotypic diversification with varying levels of extinction, and an evaluation of Type I and Type II error rates.

To test the sensitivity of our methods to unsampled past extinction events, we first simulated birth-death phylogenies using various levels of extinction. In particular, we fixed the birth rate at $\lambda = 1.0$ and simulated 1,000 trees at each of various death rates ($\mu = 0.0$, 0.1, 0.3, 0.5, 0.7, and 0.9). We simulated phylogenies containing 100 extant taxa to match our empirical phylogenetic tree of Greater Antillean anoles. For very high levels of extinction, our phylogenetic simulations often went extinct or left fewer than 100 extant taxa. When this occurred, we discarded the tree and repeated the simulation until we found a tree with 100 extant species. Next, we pruned from our trees all extinct lineages diverging below the node containing the common ancestor of all the extant lineages. This is because those lineages do not represent unsampled extinct lineages from our crown group. We note that it is of course possible that extinct lineages originating prior to the crown group influenced the evolutionary history of our study clade. However, no existing phylogenetic method (e.g., Bokma 2008) incorporates extinct lineages that do not originate from a sampled branch in the reconstructed phylogeny, thus we think it is fair to exclude them from our study. In the case of anoles, unsampled extinct lineages originating below the crown group of Greater Antillean anole fauna probably would have consisted of taxa from the Lesser Antilles or on the Central or South American mainland, so they would not have been likely to have influenced the evolution of the species in the present study.

Next, we simulated phenotypic evolution on our random birth-death phylogenetic trees under three models and four sets of model conditions. We simulated evolution that declined as a function of lineage diversity, with generating parameter values for this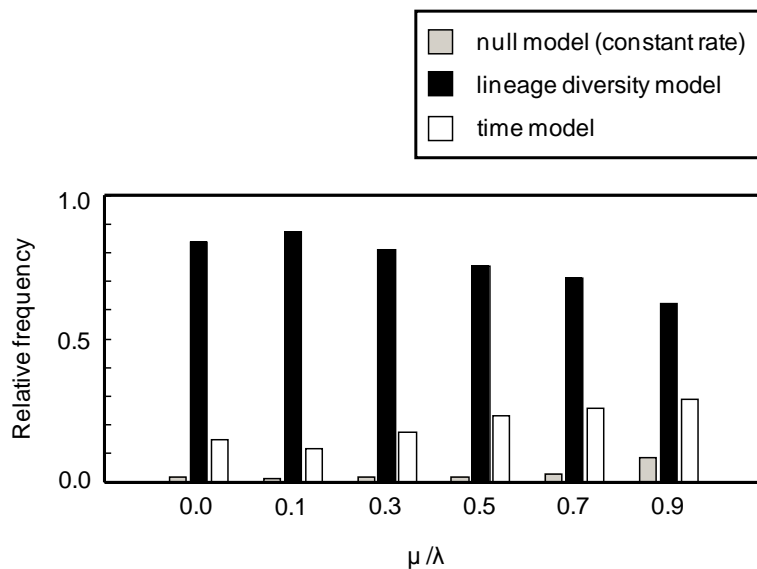 model derived from our best fitting model of phenotypic evolution for body size (SVL) in anoles (which was the lineage diversity model); we also simulated constant evolution with parameter values from our null model for body size evolution. We simulated evolution that declined as a function of time since the root node of the tree, with generating parameter values derived from our best fitting model of phenotypic evolution for PC I (limbs) in anoles (which was the time model); we also simulated constant rate evolution with parameter values from our null model for PC I evolution. Note that we simulated only diversity or time-dependent evolution, and ignored the inter-island biogeographic scenarios which also formed a part of our models in the main article. This is because the
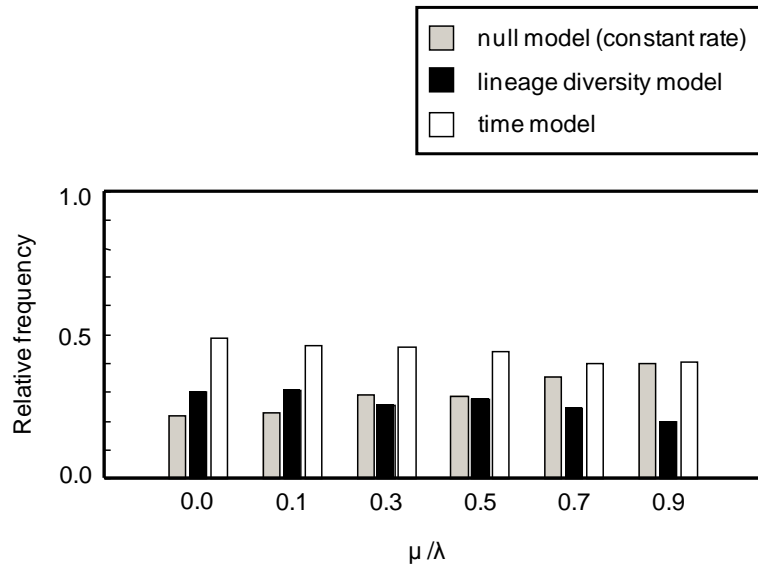

Figure S2. Model selection results for various levels of μ / λ **(extinction/speciation), with** $\lambda = 1.0$ **in all simulations. The lineage diversity model is the generating model of phenotypic evolution.**

Figure S3. Model selection results for various levels of μ / λ **(extinction/speciation), with** $\lambda = 1.0$ **in all simulations. The time model is the generating model of phenotypic evolution.**
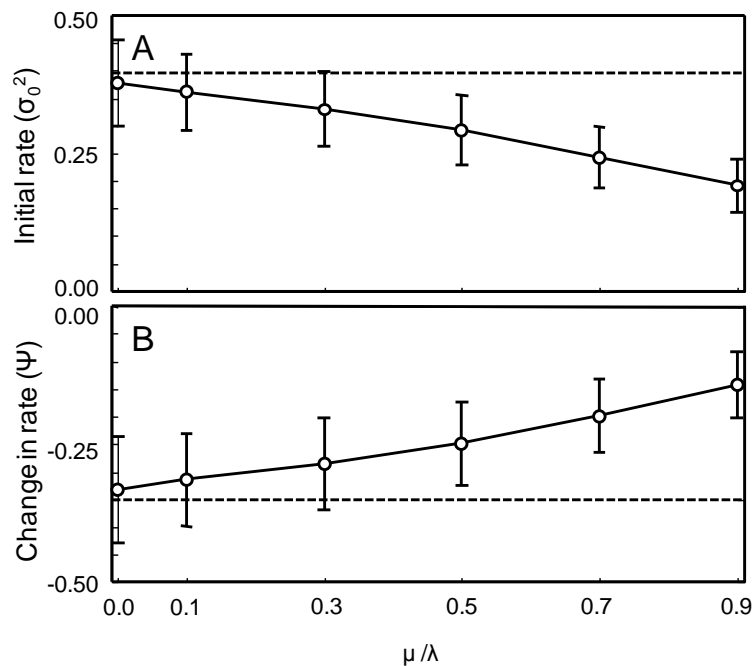

Figure S4. Parameter estimation for the lineage diversity model with increasing levels of extinction. A) Parameter estimation for the initial rate (σ_0^2 **) from the lineage diversity simulations, for various levels of extinction (** μ / λ **, for** $\lambda = 1.0$ **). B) Parameter estimation for the change in rate for each additional lineage (** $\psi \times 10^2$ **), for various levels of extinction. The horizontal dashed line is the generating parameter value, and the error bars are the standard deviation of the distribution of estimates from 1,000 numerical simulations.**

focus of these supporting analyses is on the sensitivity of our models to extinction, and we felt that this could be assessed without also simulating complex biogeography.

Then, we fit all three of our models (constant rate, lineage diversity, and time) to data generated under the four model/simulation conditions described above. We computed model selection criteria (AICc) for each fitted model when the diversity-dependent or time-dependent generating conditions were used. To analyze Type I error, we also computed likelihood ratios and P-values for the constant rate simulations evaluated using the lineage diversity or time models.

Figure S2 shows model selection proportions for data generated by the lineage diversity model. Regardless of the extinction rate, the correct model (lineage diversity) was overwhelmingly favored. The fraction of simulations in which the lineage diversity model was selected declined slightly for increased extinction rates, corresponding with a slight increase in incorrect selection of the time model.

Figure S3 shows model selection proportions for data generated under the time model. Again, regardless of extinction rate, the correct generating model (time) was favored most commonly. We found that the lineage diversity model was also frequently selected for low extinction simulations. We think that this probably represents a difficulty in distinguishing time from lineage diversity when the effect size is small – although we are unsure as to why this did not similarly affect our analyses when lineage diversity was the generating model. We note that there is a tendency to increasingly favor the null model for higher levels of extinction.

Figure S4 shows parameter

estimation in the lineage diversity model for increasing levels of extinction. We estimated two parameters of interest in the lineage diversity model: σ_0^2, the starting rate of evolution at the root node when lineage diversity is lowest; and ψ, the per-lineage rate of decrease in the evolutionary rate as lineages accrue. We found that parameter estimates for both σ_0^2 and ψ were nearly completely unbiased when no extinction was simulated, but became progressively biased toward 0.0 for increased levels of extinction.

Figure S5 shows parameter estimation in the time model for increasing levels of extinction. Again, we estimated two parameters: σ_0^2, the starting rate at the root of the tree; and ψ the rate of decrease in the evolutionary rate over time. Note that parameter estimation and model selection are also affected by extinction in this model. This is because the relevant measure of time for the evolutionary rate of a given lineage in our model is the height of its parent node above the root. When

Figure S5. Parameter estimation for the time model with increasing levels of extinction. A) Parameter estimation for the initial rate (σ_0^2) from the time heterogeneous simulations, for various levels of extinction (μ/λ , for $\lambda = 1.0$). B) Parameter estimation for the change in rate over time (ψ), for various levels of extinction. The horizontal dashed line is the generating parameter value, and the error bars are the standard deviation of the distribution of estimates from 1,000 numerical simulations.

the tree contains many unseen internal nodes (for example, when the rate of extinction is high), then a single branch will have experienced many different evolutionary rates, causing our parameter estimates based on the phylogeny of only extant taxa to be biased. For this model, we find that the parameter estimates are slightly biased towards 0.0 even when there is no extinction, as is common for maximum likelihood estimates (Lynch and Walsh, 1998). However, we also find that this bias does not become much more severe as extinction is increased.

Figure S6 shows Type I error of both models when the data were generated under the null hypothesis. The lineage diversity model never has Type I error that was statistically distinguishable from the nominal level of 0.05. However, the time model had significantly elevated Type I error for both the lowest non-zero level of extinction ($\mu = 0.1$) and for the highest extinction level ($\mu = 0.9$).
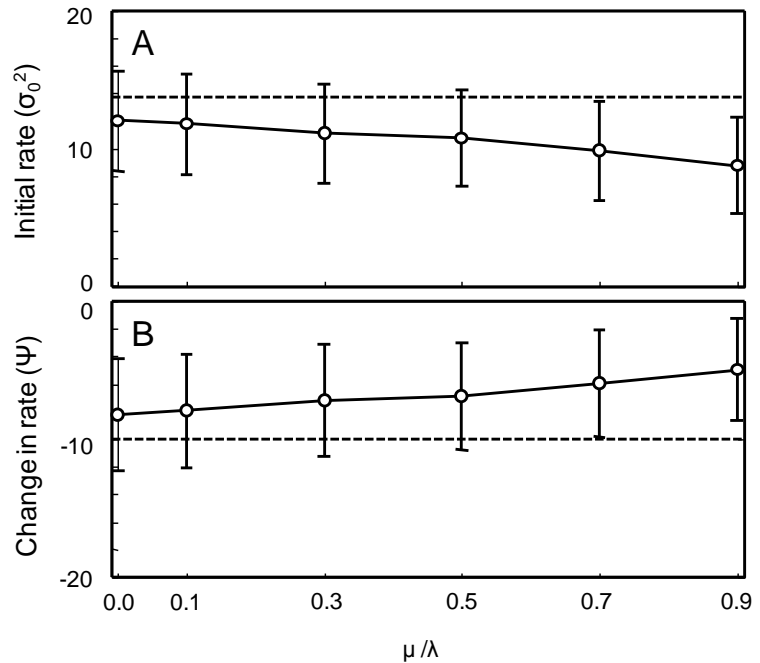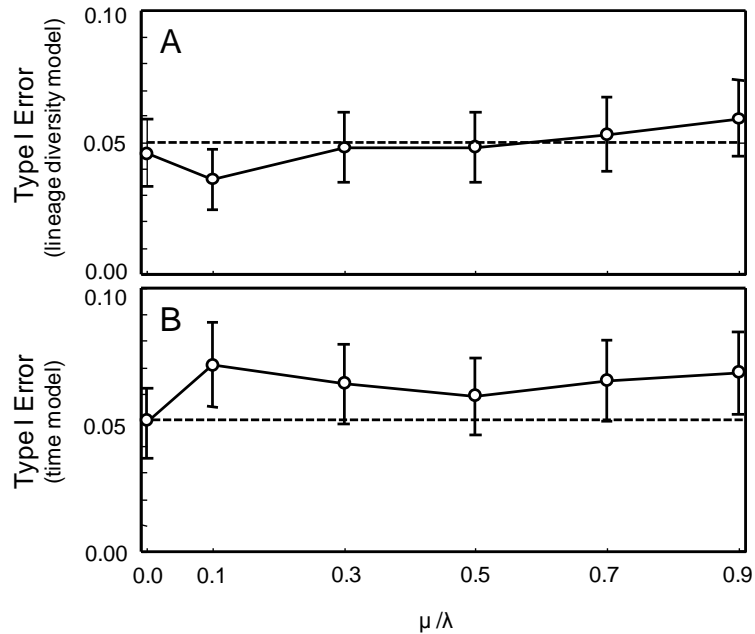
Figure S6. Type I error rates for the lineage diversity and time models with increasing levels of extinction. A) Type I error of the lineage diversity model, when the simulated model was a constant rate model, for various levels of extinction (μ / λ , for $\lambda = 1.0$). B) Type I error of the time model, for various levels of extinction. The horizontal dashed line is the nominal Type I error rate, and the error bars are the 95% confidence interval for the Type I error proportion from 1,000 numerical simulations.

APPENDIX S3: QUANTIFYING SIMILARITY OF PRINCIPAL COMPONENT AXES AMONG THE PHYOLOGENIES USED IN OUR ANALYSES

All of our comparative analyses, including our phylogenetic principal component analyses, were conducted on each of 898 phylogenies sampled from the posterior distribution of Bayesian analysis (see Methods). However, the degree to which the results of our rate tests from different trees are comparable for traits PC I – IV depends on how similarly these four axes are aligned across different phylogenies (e.g., in theory, toe pad width may load heavily on PC III in one analysis while head height loads heavily on PC III in a different analysis, in which case patterns of evolution for PC III would not be comparable across analyses). To quantify the alignment of the subspaces defined by the first four principal component axes across our sample of phylogenies, we used the method of Krzanowski (1979). With this method, the maximum alignment between two subspaces is the dimensionality of the spaces (which is equivalent to the number of eigenvectors analyzed - four in this case). We found that the average subspace alignment of principal component analysis performed from all 898 trees in our posterior sample was 3.82. Furthermore, the minimum subspace alignment between eigenvectors calculated in PCA performed on the MCC tree and any tree from our sample of the posterior distribution was 3.46, which is still quite close to four, meaning that these four axes are very similar across phylogenies. Given the high similarity of phylogenetic eigenanalyses performed on all sampled trees in the posterior distribution to the PCA performed on the MCC tree, we only present information from the latter in Table 1.

APPENDIX S4: THE RELATIONSHIP BETWEEN ECOLOGICAL OPPORTUNITY AND RATES OF EVOLUTION FOR TRAIT AXES PC II – IV
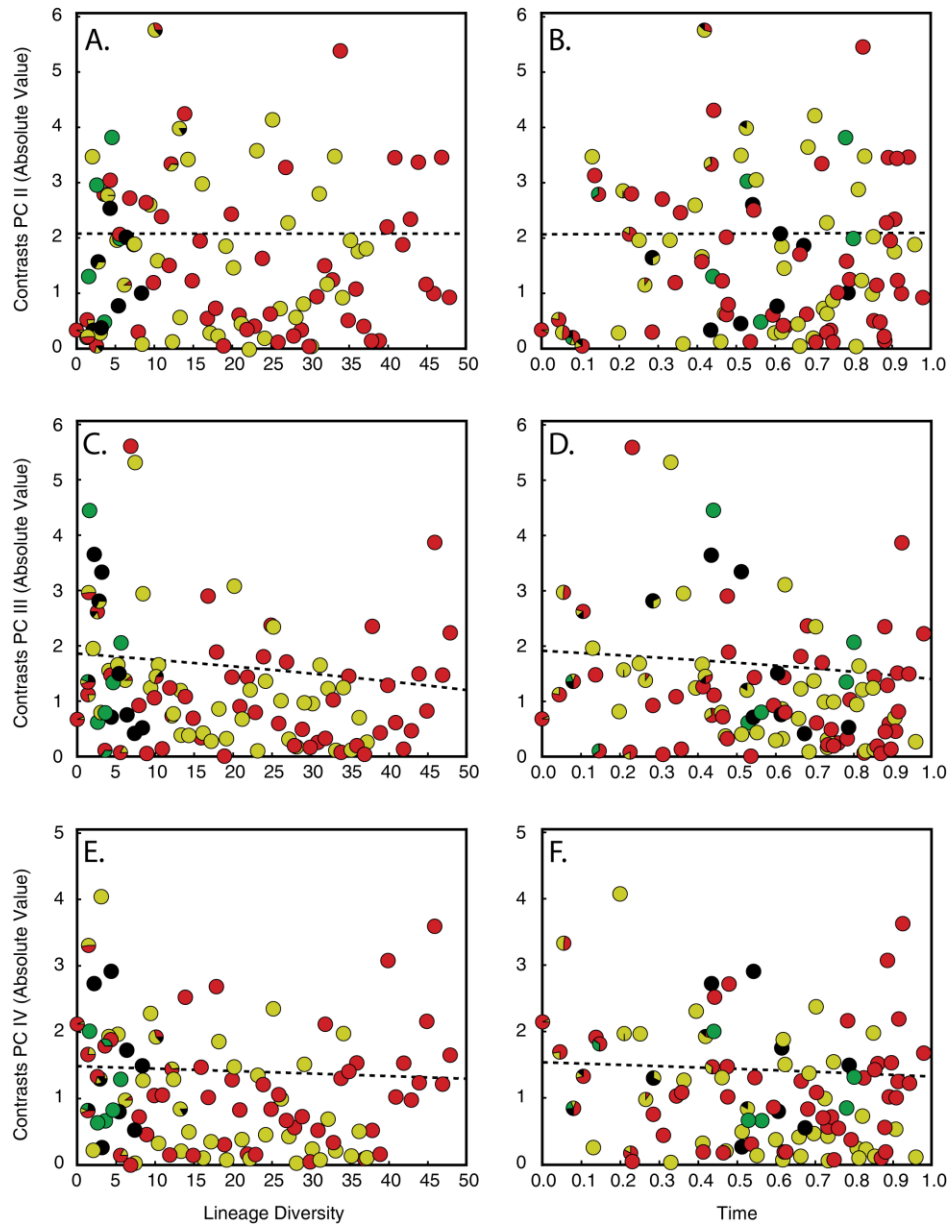

Figure S7. Absolute values of standardized phylogenetically independent contrasts of morphological traits for the Bayesian MCC phylogeny of Greater Antillean *Anolis*. A) and B) show PC II contrasts with increasing lineage diversity and relative time, respectively. C) and D) show PC III contrasts with increasing lineage diversity and relative time, respectively. E) and F) show PC IV contrasts with increasing lineage diversity and relative time, respectively. Dashed lines show the expected standard deviation under the best-fit model in which the evolutionary rate varied as a function of the number of lineages (left panels) or time (right panels). Colors represent the islands on which nodes occurred, estimated using maximum likelihood (red is Cuba; yellow is Hispaniola; black is Puerto Rico; green is Jamaica).

APPENDIX S5: DISCUSSION OF ADDITIONAL MODEL ASSUMPTIONS AND POTENTIAL BIASING FACTORS

Here we discuss additional potential sources of error that should be considered when applying our methods for estimating ecological opportunity and testing for a relationship between opportunity and rate. None of these are problematic for the present study; however they should be considered in future studies utilizing our approach. We outline several issues here, discussing the nature of each problem, and its specific relationship to the present study on Greater Antillean anoles.

1) Lineage Density Estimation

In the present study, we assume that ecological opportunity decreases monotonically with increasing island lineage diversity, but local community ecological opportunity may influence phenotypic diversification more than whole-island ecological opportunity. For example, no single Greater Antillean anole community has more than 15 species, yet lineage diversity on Hispaniola and Cuba reaches values of 41 and 63 respectively (our estimates were slightly lower due to the unavailability of some species for study). Although regional species richness may contribute to the regulation of rates of phenotypic evolution, community level species competition may be more important. We note that our method for estimating whole-island lineage diversities is not inconsistent with community diversity on those islands, because larger islands tend to have richer communities. Thus, island and local community diversities correspond, but the island diversities increase at a more rapid rate.

To explore the potential relationship between community lineage diversity and the rate of evolution, we repeated our lineage diversity analysis for SVL and PC I after natural log-transforming our lineage diversity estimates, which has the effect of deflating the higher per-island diversity estimates relative to the lower ones (note – we first added 1 to our estimates to avoid obtaining negative transformed values). The transformed lineage diversity model received a similar level of support as the standard lineage diversity model (Table S1). We are reluctant to over-interpret these results, as we consider our choice of a natural log transformation to be ad hoc, but the performance of this model is encouraging for the ecological opportunity hypothesis. Future work may be directed towards further refinement of such measures of historical ecological opportunity.

Table S1: Comparison of models of rate variation, including ln-transformed lineage diversity. All values represent results averaged from 898 topologies sampled randomly from a Bayesian posterior distribution.

Trait	Model	σ_0^2	ψ	$\log(L)$	ΔAIC_c	AIC_c weight
size (SVL)	single rate	0.14	-	-42.67	7.44	0.02
	time	0.25	-0.18	-40.69	5.57	0.06
	lineage diversity	0.20	-3.5E-3	-38.02	0.23	0.51
	ln(lineage diversity)	0.34	-0.07	-38.28	0.76	0.41
PC I	single rate	7.75	-	-241.86	4.04	0.10
	time	13.68	-10.04	-238.80	0.00	0.59
	lineage diversity	10.06	-0.12	-240.19	2.80	0.14
	ln(lineage diversity)	14.62	-2.52	-240.03	2.46	0.17

2) Sampling Error

Next, our methods do not account for the potential influence of sampling error in the estimation of species means for traits. Sampling error will tend to inflate the variance of recent contrasts relative to deeper contrasts in the phylogeny because deeper contrasts in the tree are calculated between weighted averages of the taxa above the contrasted nodes, and thus will be less susceptible to error in species values than will be more recent contrasts, many of which will be calculated using species values themselves. Figure S8 shows the results from the best-fit model for evolutionary rate and lineage diversity or time for data simulated under a constant rate evolutionary process with sampling error in the estimation of species values. With sampling error, the lineage diversity model recovered an increasing rate of phenotypic evolution of 0.17 trait units per additional lineage; this model was significantly favored over a single rate model using a likelihood ratio test (p = 0.004; results averaged from 100 simulations). Also, the time model recovered an increasing rate of phenotypic evolution of 6.88 trait units per unit time, a model which was significantly favored over a single rate model using a likelihood ratio test (p = 0.002). Because the artifact due to sampling error results in the opposite pattern to the opportunity hypothesis (i.e., increasing evolutionary rate through time), we do not consider it to be an important source of bias for investigations testing for patterns of decreasing rates of phenotypic evolution with lineage diversity or time. However, future authors interested in testing for increasing evolutionary rate through time should be aware that this pattern can be induced as an artificial consequence of intraspecific sampling error. Felsenstein's (2008) contrasts method incorporating within-species variation might provide an appropriate remedy to this problem, but we have not explored this possibility. Finally, we note that Type II error due to sampling error is expected to more strongly affect detection of ecological opportunity in less variable traits (e.g., PC axes with lower eigenvalues) because the signal-to-noise ratio will be lower for such data.
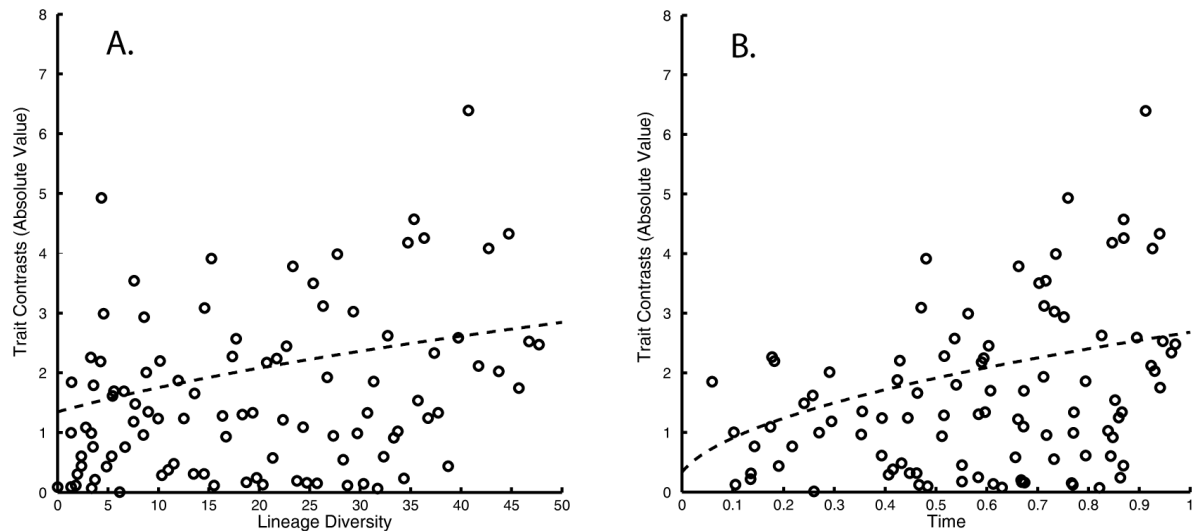

Figure S8. Standardized phylogenetically independent contrasts of traits simulated under a Brownian motion model of evolution using a representative phylogeny of Greater Antillean *Anolis*, with randomly generated sampling error. A) and B) show trait contrasts with increasing lineage diversity and relative time, respectively. Dashed lines show the expected standard deviation of the contrasts under the best-fit model in which the evolutionary rate varies as a function of the number of lineages (A) or time (B).

3) Branch Length Estimation

Our methods also assume that the branch lengths in the tree have been estimated without bias. Any bias towards underestimating the lengths of deep branches in the tree (e.g., Revell et al. 2005) will tend to inflate phenotypic rate estimates for these branches, producing a pattern akin to the temporal slowdown we observed empirically (Figure 4). Although this problem warrants further consideration, such bias would be expected to afflict all characters equally, but we detected no pattern of decreasing evolutionary rate through time for PCs II-IV (Table 2; Figure S7).

4) Evolution Associated with Colonization Events

Our lineage density model tests whether rates of phenotypic evolution are elevated when diversification occurs in a novel environment – for example, when diversification occurs after colonization of a new island. However, an alternative possibility is that evolutionary change is most rapid in the colonizing lineage (which finds itself in a new landscape), as opposed to its first descendents (which split in the presence of new opportunity). If evolution was most pronounced in colonizing lineages, this should most strongly influence the independent contrast values of the nodes preceding colonization events.

We tested whether such a colonization-associated pattern may have influenced our model comparison results by reanalyzing our data after removing nodes preceding colonization events. Because the early colonization history of the Greater Antilles is somewhat uncertain, choosing which nodes to remove was difficult. To be conservative, we tried a range of possibilities (as few as four and as many as seven, in which case all such potential nodes were removed). In all cases, our method recovered the same general pattern previously observed for size (SVL) and limb shape (PC I), and in all cases, support for the previously favored model (lineage diversity for SVL; time for PC I) was actually stronger than when these earlier nodes were included (see Table S2, which includes results for the two trait axes for which ecological opportunity models were favored).

Table S2: Comparison of models of rate variation with 'pre-colonization' nodes removed for SVL and PC I, using the MCC tree. These results were obtained after removing seven nodes in which one descendant potentially occurred on a different island than its ancestor. Other combinations of nodes were removed, but all results were similar to those presented here, and in all instances, model selection results match those presented in our manuscript (Table 2).

Trait	Model	σ_0^2	ψ	$\log(L)$	ΔAIC_c	AIC_c weight
size (SVL)	single rate	0.14	-	-39.81	11.02	0.00
	Time	0.25	-0.18	-38.45	10.38	0.01
	lineage diversity	0.22	-4.1E-03	-33.26	0.00	0.99
PC I	single rate	7.75	-	-221.87	8.05	0.02
	Time	15.47	-13.39	-216.80	0.00	0.88
	lineage diversity	10.38	-0.15	-218.97	4.35	0.10

APPENDIX S6: SUPPLEMENTARY LITERATURE CITED

Bokma, F. 2009. Problems detecting density-dependent diversification on phylogenies. Proc. R. Soc. B 276:993-994.

de Queiroz, K., L. Chu, and J. B. Losos. 1998. A second *Anolis* lizard in Dominican amber and the systematics and ecological morphology of Dominican amber anoles. Am. Mus. Novit. 3249:1-23.

Felsenstein, J. 1985. Phylogenies and the comparative method. Am. Nat. 125:1-15.

Felsenstein, J. 2008. Comparative methods with sampling error and within-species variation: contrasts revisited and revised. Am. Nat. 171:713-725.

Kubo, T., and Y. Iwasa. 1995. Inferring the rates of branching and extinction from molecular phylogenies. Evolution 49:694-704.

Lynch, M., and J. B. Walsh. 1998. Genetics and analysis of quantitative traits. Sinauer Assocs. Inc., Sunderland, MA.

Marshall, C. R. 2007. Explaining latitudinal diversity gradients. Science 317:451-452.

McPeek, M. A. 2008. The ecological dynamics of clade diversification and community assembly. Am. Nat. 172:E270-E284.

Mooers, A. Ø., and S. B. Heard. 1997. Inferring evolutionary process from phylogenetic tree shape. Q. Rev. Biol. 72:31-54.

Nee, S., E. C. Holmes, R. M. May, and P. H. Harvey. 1994. Extinction rates can be estimated from molecular phylogenies. Philos. Trans. R. Soc. Lond. B Biol. Sci. 344:77-82.

Polcyn, M. J., J. V. Rogers II, Y. Kobayashi, and L. L. Jacobs. 2002. Computed tomography of an *Anolis* lizard in Dominican amber: systematic, taphonomic, biogeographic, and evolutionary implications. Palaeontol. Electronica 5:1-13.

Pybus, O. G., and P. H. Harvey. 2000. Testing macro-evolutionary models using incomplete molecular phylogenies. Proc. R. Soc. B 267:2267-2272.

Quental, T. B., and C. R. Marshall. 2009. Extinction during evolutionary radiations: reconciling the fossil record with molecular phylogenies. Evolution 63:3158-3167.

Rabosky, D. L., and I. J. Lovette. 2008a. Explosive evolutionary radiations: decreasing speciation or increasing extinction through time? Evolution 62:1866-1875.

Rabosky, D. L., and I. J. Lovette. 2008b. Density-dependent diversification in North American wood warblers. Proc. R. Soc. B 275:2363-2371.

Rabosky, D. L. 2009a. Ecological limits and diversification rate: alternative paradigms to explain the variation in species richness among clades and regions. Ecol. Lett. 12:735-743.

Rabosky, D. L. 2009b. Heritability of extinction rates links diversification patterns in molecular phylogenies and fossils. Syst. Biol. 58:629-640.

Rabosky, D. L. 2010. Extinction rates should not be estimated from molecular phylogenies. Evolution Early View doi:10.1111/j.1558-5646.2009.00926.x.

Revell, L. J., L. J. Harmon, and R. E. Glor. 2005. Underparameterized model of sequence evolution leads to bias in the estimation of diversification rates from molecular phylogenies. Syst. Biol. 54:973-983.

Rieppel, O. 1980. Green anole in Dominican amber. Nature 286:486-487.